Mechanical loss of a hydroxide catalysis bond between sapphire substrates and its effect on the sensitivity of future gravitational wave detectors

K. Haughian,[1,*] D. Chen,[2] L. Cunningham,[1] G. Hofmann,[3] J. Hough,[1] P. G. Murray,[1] R. Nawrodt,[3] S. Rowan,[1] A. A. van Veggel,[1] and K. Yamamoto[2]

[1]*SUPA, School of Physics and Astronomy, University of Glasgow, Glasgow G12 8QQ, United Kingdom*
[2]*Institute for Cosmic Ray Research (ICRR), The University of Tokyo, 5-1-5, Kashiwanoha, Kashiwa, Chiba 277-8582*
[3]*Institut für Festkorperphysik, Friedrich-Schiller-Universität, Jena, Helmholtzweg 5, D-07743 Jena, Germany*

(Received 19 August 2016; published 12 October 2016)

Hydroxide catalysis bonds are low mechanical loss joints which are used in the fused silica mirror suspensions of current room temperature interferometric gravitational wave detectors, one of the techniques which was essential to allow the recent detection of gravitational radiation by LIGO. More sensitive detectors may require cryogenic techniques with sapphire as a candidate mirror and suspension material, and thus hydroxide catalysis bonds are under consideration for jointing sapphire. This paper presents the first measurements of the mechanical loss of such a bond created between sapphire substrates and measured down to cryogenic temperatures. The mechanical loss is found to be 0.03 ± 0.01 at room temperature, decreasing to $(3 \pm 1) \times 10^{-4}$ at 20 K. The resulting thermal noise of the bonds on several possible mirror suspensions is presented.

DOI: 10.1103/PhysRevD.94.082003

I. INTRODUCTION

Large scale interferometric detectors have observed two gravitational wave signals thus facilitating the dawn of gravitational wave astronomy [1,2]. Both of these gravitational wave events, the first detected on September 14, 2015 [1], and the second detected on December 26, 2015 [2], were created by black hole binary mergers and were observed by both LIGO detectors in the USA [3,4]. Other gravitational wave detectors include GEO600 in Germany [5,6], which is operational, and Virgo, in Italy [7,8], which is currently being upgraded. These detectors have been developed and upgraded to achieve a sensitivity level at which gravitational waves coming from astrophysical sources can be detected [3–8]. As the sensitivities of the detectors are improved, the number of observable events increases. Many noise sources limit the sensitivity of the detectors, one of the dominant noise sources being the thermal noise of the mirror suspensions [9]. In the development and upgrades of the current detectors, many techniques have been employed to reduce the level of thermal noise. These include the careful selection of the low mechanical loss material fused silica for the mirrors and their suspension elements [3,6,8,10], the selection and optimization of the mirror coatings [11], the suspension fiber design [12], and the use of hydroxide catalysis bonding to chemically join the suspension components [13,14]. All of these elements were crucial in obtaining the first detection.

For possible future upgrades to these detectors and for new detectors, such as the detector in Japan, KAGRA [15,16], and the European detector concept, the Einstein Telescope (ET) [17–19], the cooling of the suspension down to cryogenic temperature may be employed as a method of reducing the level of thermal noise [20,21]. At low temperature, ~40 K, fused silica exhibits high levels of dissipation, and therefore an alternative mirror and suspension material is required [22]. Sapphire has been under consideration as an alternative material for many years [23–27]. The KAGRA Collaboration has selected sapphire as the mirror and suspension material [15,16] for their detector under the Kamioka mountain, while silicon is currently the baseline material for that part of the Einstein Telescope operating at lower frequencies [17–19]. However, sapphire is a potential alternative candidate material for ET. A full understanding of the suspension and its elements at low temperatures is required in order to evaluate the level of thermal noise that will be present and hence the possible increase in performance possible with future instruments.

A feasibility study is underway for the use of hydroxide catalysis bonding in jointing crystalline materials in gravitational wave detector mirror suspensions [28–33]. Indium bonding is also being investigated; however, indium bonds would only be used in compressive load conditions [34,35]. It has previously been demonstrated that the hydroxide catalysis bonding technique can provide bonds (silicon-silicon and sapphire-sapphire) with the strength required

*Corresponding author.
karen.haughian@glasgow.ac.uk

for these suspensions at both room and cryogenic temperatures, and, here, the suitability of a sapphire-sapphire bond to a gravitational wave detector suspension in terms of noise is investigated. The mechanical loss at several resonant frequencies of two sapphire cylinders (one reference sample and one containing a hydroxide catalysis bond) in the temperature range ~5–310 K is presented. Finite element models showing the motion of the cylinders at each of their resonant frequencies were created showing the ratio of the energy stored in the bond to the energy stored in the sapphire samples. This energy ratio was used to extract the mechanical loss of the hydroxide catalysis bond from the mechanical loss results of the samples. The mechanical loss is then used in models of potential sapphire suspension designs to predict the thermal noise introduced by the bonds.

II. HYDROXIDE CATALYSIS BONDING

A hydroxide catalysis bond is a chemical joint created using a hydroxide bonding solution to synthesize silicate. This technique was first created by Gwo for use in the Gravity Probe B satellite [36–38]. It has since been further developed for use in the construction of ground- and space-based gravitational wave detectors [13,32,33,39–41].

A. Chemistry

As described in Refs. [36,38], when an alkali hydroxide bonding solution comes into contact with fused silica surfaces, a hydroxide catalysis bond is formed in three main steps: hydration (and etching), polymerization, and dehydration. The bonds connecting the mirror suspension components in aLIGO and GEO600 used a sodium silicate bonding solution. The hydroxide etches the surfaces releasing silicate molecules, $Si(OH)_5$, from the bulk material into the bonding solution. Once the pH of the bonding solution drops below 11, the silicate molecules dissociate to form siloxane, $Si(OH)_4$ [42]. The siloxane begins to form siloxane polymer chains and water. The water evaporates or migrates out of the bond over a four week curing period after which the bond has reached its full strength [13,39,43]. The chemical form and structure of the bond is shown in Eq. (1):

$$(HO)_3SiOSi(OH)_3. \quad (1)$$

The chemistry of a bond created between sapphire substrates differs as sapphire cannot form a silicatelike network of its own but can attach to an existing one to form an aluminosilicate network. This is thought to consist of a mixture of aluminate chains and siloxane chains [44]. A potential chemical form and structure of a sodium hydroxide bond created between sapphire substrates is shown in Eq. (2):

$$(HO)_2AlOSi(OH)_3. \quad (2)$$

For strong bonds to be formed, the surfaces to be bonded must be clean [38]. Thus, a strict cleaning procedure is carried out on the surfaces in progressive steps using cerium oxide and deionized water, sodium bicarbonate and deionized water, and methanol, respectively [45]. This prevents contamination in the bond and makes the surfaces hydrophilic, allowing the bonding solution to freely spread out over the whole bonding area. Another requirement for strong bonds is that the two bonding surfaces must be able to come sufficiently close enough to each other to allow the chemical process to take place and form a thin bond. Thus, a global peak to valley flatness of $\lambda/10$ (where $\lambda = 633$ nm) is desirable [39]. The thickness of a bond created between silica samples of this flatness is typically (61 ± 4) nm [14,46].

B. Samples and crystal alignment

A schematic diagram of all three single crystal sapphire samples studied is shown in Fig. 1. All the samples had a (30 ± 0.1) mm diameter, and they were (120 ± 0.1) mm (reference sample), (70 ± 0.1) mm, and (50 ± 0.1) mm long, respectively. They were manufactured by Impex[1] such that the cylindrical axis of each sample was parallel to the c axis of the sapphire crystal. The samples were inspection polished with the exception of one end face on each of the two shorter samples which was specified to have a global peak to valley flatness of $\lambda/10$ where $\lambda = 633$ nm. These surfaces were used as the bonding surfaces. A Logitech[2] LI10 interferometer was used to image the two bonding surfaces and allow the flatness to be calculated to be (70 ± 5) nm on the 70 mm long sample and (79 ± 5) nm on the 50 mm long sample. Finite element models were created using ANSYS[3] in order to investigate the effect that a misalignment of the a and m crystal orientation of the two samples would have on the frequency and distribution of motion of the resonant modes of the bonded sample. One sample was rotated with respect to the other, and the resultant frequencies and ratio of the energy stored in the bond to the energy stored in the bulk substrates were recorded. This was repeated for several rotations, and the change in the frequency and energy ratio values was less than 1%. Therefore, aligning the m axis or a axis of the crystal before bonding was not of great importance.

C. Bonding procedure

The bonding solution was formed using a commercially available sodium silicate solution (14% sodium hydroxide, 27% silicate, and 59% deionized water). This was diluted, one part sodium silicate solution to six parts deionized

[1] www.impex-hightech.de
[2] www.logitech.com
[3] www.ansys.com

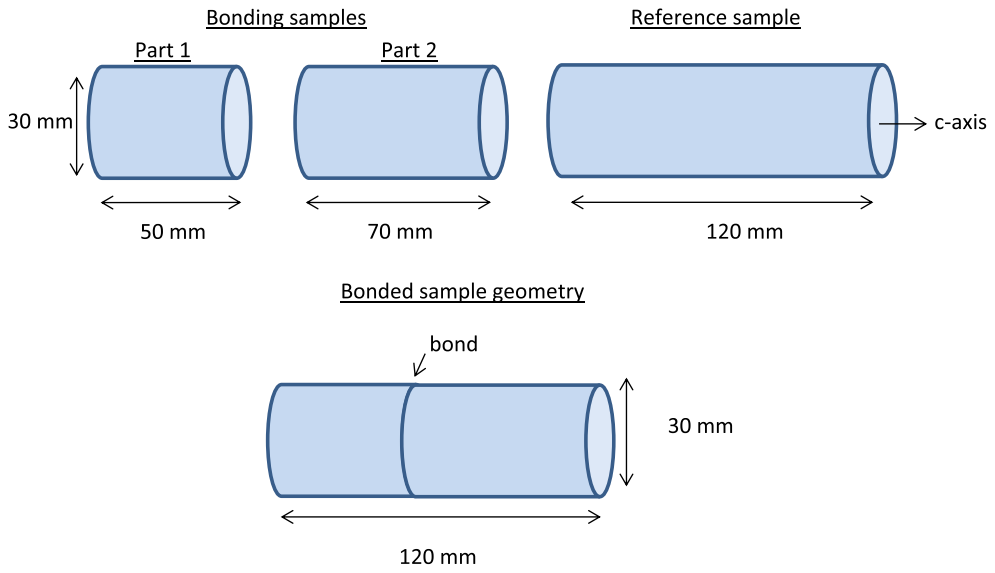

FIG. 1. Schematic diagram of the sapphire samples studied before and after hydroxide catalysis bonding. All the samples have a diameter of 30 mm, and the cylindrical axis of the sample is the c axis of the sapphire crystal. The reference sample is 120 mm long, and the two samples that were bonded together were 50 and 70 mm long, respectively.

water. The solution was then shaken vigorously for around 60 s. The mixed solution was poured in equal measures into three 1.5 ml centrifuge tubes and centrifuged for around 60 s. A portion of the solution was then filtered using a 0.2 μm medical filter.

The samples were cleaned using the standard cerium oxide, sodium bicarbonate, and methanol procedure before bonding [45]. The last step before bonding was to wipe the surfaces once using a clean room cloth which had been wetted with $> 99.9\%$ pure methanol. They were then inspected with a high intensity lamp to ensure that there were no contaminants present on the surfaces. A volume of 2.83 μl (0.4 μl/cm^2 of bonding surface) of bonding solution was placed on the 50 mm sample bonding surface using a pipette, and the bonding surface of the 70 mm sample was brought into contact by placing the 70 mm sample on top. The bonded sample was left to cure for four weeks at room temperature.

III. MECHANICAL LOSS MEASUREMENTS

The sample to be measured was suspended inside a cryostat with a loop of 35 μm diameter tungsten wire as shown in Fig. 2. The cryostat provided the cooling power required to reduce the temperature of the sample to the desired temperatures for measurement. The tungsten wire supported the sample while allowing it enough freedom to resonate freely when excited. A temperature sensor was placed directly onto a second suspended sapphire sample of similar volume which provided the temperature calibration for the investigated sample. The motion at the resonant frequencies was then induced by the use of an electrostatic plate driven by high voltage (up to 1600 V). This allowed the sample to be excited at each selected resonant mode in turn. After the sample started resonating with a sufficient amplitude of motion, the excitor plate was switched off and the motion of the front face of the sample was recorded using a interferometer manufactured by SIOS.[4] By monitoring the amplitude of the decaying motion, A(t), the mechanical loss can be calculated using

$$A(t) = A_o e^{-\phi(f)\pi f t}, \tag{3}$$

where A_o is the amplitude at time $t = 0$, f is the frequency of the resonant mode, and $\phi(f)$ is the mechanical loss of the material [47]. The mechanical loss of both the reference (ϕ_{sapphire}) and the hydroxide catalysis bonded sample (ϕ_{bonded}) was measured down to approximately 5 K. Using this data and the energy distribution in the sample, which was obtained from finite element analysis, the mechanical loss of the bond can be calculated. The mechanical loss of the bonded sample can be expressed as

$$\phi_{\text{bonded}} \simeq \frac{E_{\text{sapphire}}}{E_{\text{total}}}\phi_{\text{sapphire}} + \frac{E_{\text{bond}}}{E_{\text{total}}}\phi_{\text{bond}}, \tag{4}$$

where $E_{\text{sapphire}}/E_{\text{total}}$ is the amount of energy stored in the sapphire divided by the total energy in the sample and $E_{\text{bond}}/E_{\text{total}}$ is the amount of energy stored in the bond

[4] www.sios.de

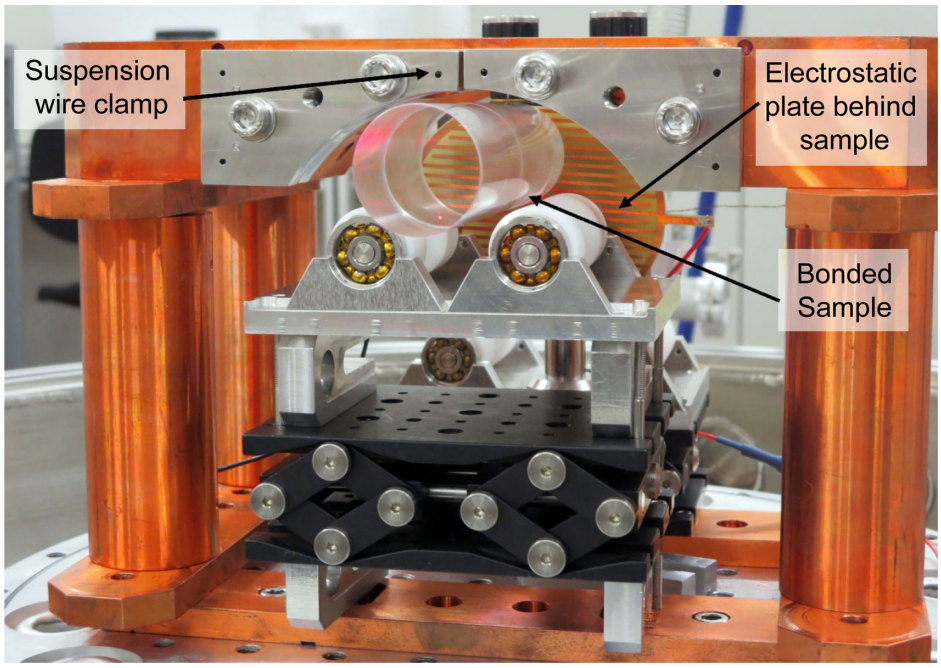

FIG. 2. Bonded sapphire rod suspended with 0.35 μm tungsten wire for mechanical loss measurements. The sample is excited by an electrostatic drive plate. As the sample rings down, the decaying motion of the front face of the sample is recorded using a SIOS interferometer. The second sapphire mass which is used for temperature calibration is suspended behind the electrostatic drive plate and so cannot be observed in this photograph.

divided by the total energy in the sample. The sapphire is substantially larger in volume than the bond, which means $E_{total} \simeq E_{sapphire}$, and therefore $E_{sapphire}/E_{total}$ is ~ 1 and can be removed from Eq. (4), which can be rearranged to give the mechanical loss of the hydroxide catalysis bond

$$\phi_{bond} \simeq \frac{\phi_{bonded} - \phi_{sapphire}}{E_{bond}/E_{total}}. \quad (5)$$

The mechanical loss of the bond was calculated for each resonant frequency. These values were averaged to give the intrinsic mechanical loss of the bond as the mechanical loss of a hydroxide catalysis bond is assumed to be independent of frequency [14].

A. Finite element modelling

In order to create a finite element model of the bonded sample, material properties of the bond and sapphire must be known. The material property values used for the bond are shown in Table I, and the material property values for sapphire were taken from Ref. [48]. The values were assumed constant through the temperature range. The density and Poisson's ratio of a hydroxide catalysis bond were assumed to be similar to that of fused silica. The Young's modulus of a hydroxide catalysis bond formed between fused silica has been previously measured to be 7.9 GPa [49]. Here, the hydroxide catalysis bond potentially has a different chemical composition due to sapphire being the bonded substrates; therefore, a 30% error on the Young's modulus of the bond was assumed [50]. (The Young's modulus of fused silica is approximately 72 GPa, and for different types of glass with different chemical compositions, the value can vary up to $\pm 30\%$ [51]). Varying the Poisson's ratio through the range typically found for glasses does not appear to have a significant effect on the results [50], and therefore it was assumed to be the same value as for fused silica, 0.17.

TABLE I. Material properties of a hydroxide catalysis bond [14,49].

	Bond material
Density (kg/m^3)	2200
Poisson's ratio	0.17
Young's modulus (GPa)	$7.9 \pm 30\%$

The finite element modelling was carried out using ANSYS[5] to directly model the bonded sample and obtain the energy ratios for the possible range of Young's modulus values of the bond [14]. The energy ratios obtained when using a Young's modulus of 7.9 GPa were cross-checked with other modelling techniques using COMSOL[6]: an extrapolation technique [14] and a thin film approach [52]. All three methods gave energy ratios in agreement with each other. The models assumed a bond thickness

[5]www.ansys.com
[6]www.comsol.ltd.uk

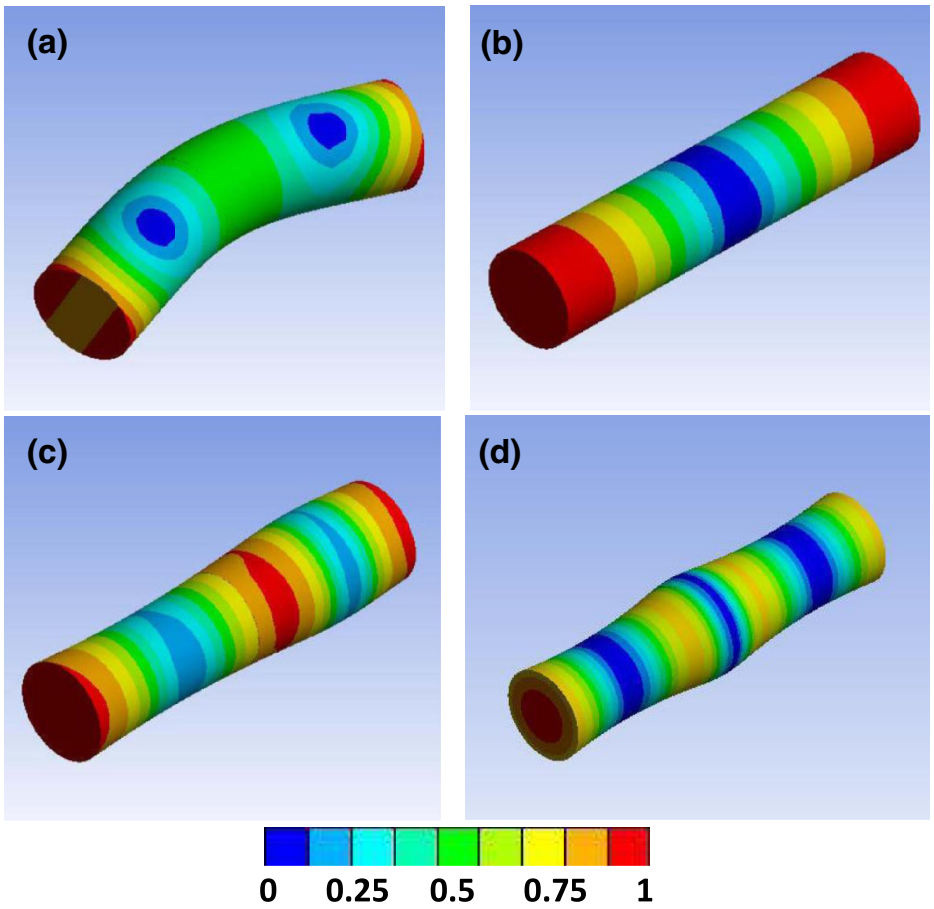

FIG. 3. Mode shapes of the four resonant frequencies at which the mechanical loss was measured. (a) 17 kHz, (b) 44 kHz, (c) 89 kHz, and (d) 132 kHz. The color indicates the relative magnitude of the motion, blue showing minimal motion and red showing maximum motion.

between 74.5 (average of the two flatnesses of the bonded surfaces) and 149 nm (sum of the two flatnesses of the bonded surfaces). Corroboration of this range was given by the examination of the surface figures through observing interferograms created on the two surfaces prior to bonding using a interferometer.[7] Bond loss values were extracted assuming both extremes of this thickness range.

IV. EXPERIMENTAL RESULTS

Before the bonding process was carried out, the mechanical losses of the individual samples were measured at room temperature as a coarse check for crystal defects in either segment that could cause excess loss. They were found to have a loss similar in magnitude to that of the reference sample and were therefore cleaned and hydroxide catalysis bonded together using the process described in Sec. II C. The bond created was optically clear over more than 95% of the bonding surface with only a few very small bubbles remaining present in the bond.

[7]www.zygo.com

The mechanical loss for four of the resonant modes of the reference and bonded samples were measured down to approximately 5 K. The mode shapes of the measured resonances are shown in Fig. 3, while the mechanical loss values obtained for both samples are shown in Fig. 4.

The mechanical losses of both of these samples decrease as the temperature is decreased, agreeing with previously published literature on the mechanical loss of sapphire [22]. The loss of the bonded sample is higher than the loss of the reference sample due to the presence of the hydroxide catalysis bond. The level of loss measured for a sample can vary depending on which resonant mode is being measured. This is due to different resonances causing motion in different areas of the sample and at different amplitudes. For modes where a large amount of energy is stored in the bond region or around the suspension region, a higher mechanical loss will be measured due to the amplification of the effect of the bond or due to frictional suspension losses. This can be seen for the 17 kHz resonant mode. A higher loss is measured for the bonded sample at this frequency as this is a bending mode, and therefore more

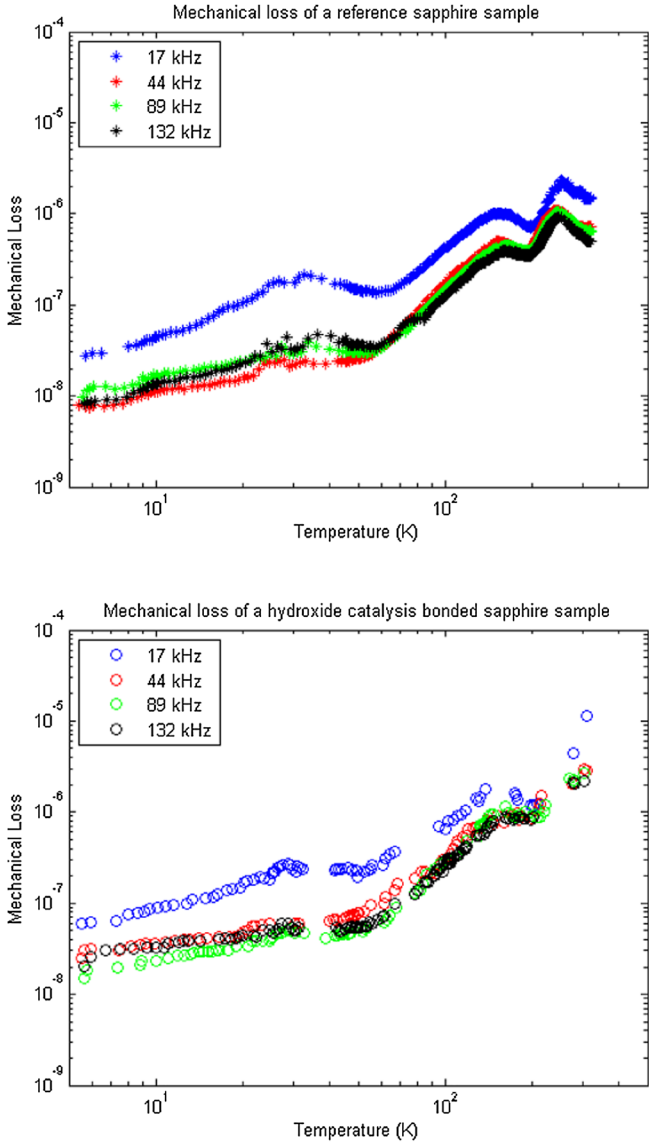

FIG. 4. Mechanical loss of sapphire samples. Top: A reference sample (30 mm diameter, 120 mm long, and a cylindrical axis cut along the c axis of the crystal). Bottom: A hydroxide catalysis bonded sapphire sample (50 mm long sample bonded to a 70 mm long sample, both having a 30 mm diameter, and the cylindrical axis cut along the c axis of the crystal). The mechanical losses of both samples were measured at four resonant frequencies.

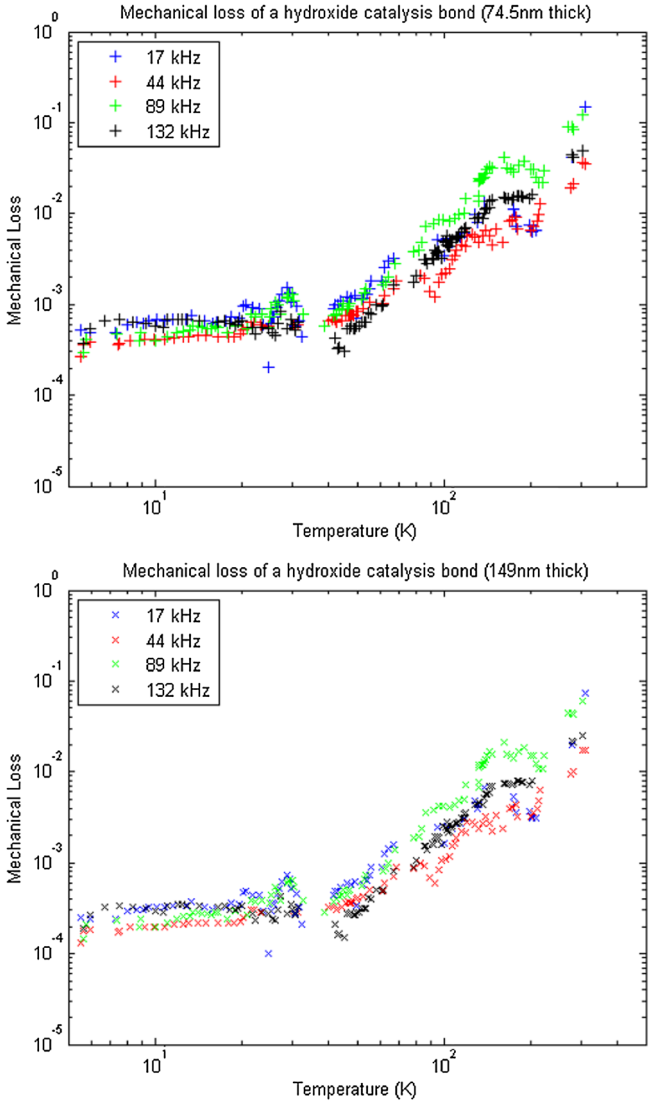

FIG. 5. Extracted mechanical loss of a hydroxide catalysis bond created between sapphire substrates assuming a 74.5 nm thick bond (top) and a 149 nm thick bond (bottom). The bond loss has been measured for four resonant frequencies. The data shown assume the Young's modulus of the bond to be 7.9 GPa.

energy is stored around the center of the sample close to the bond region.

Peaks can be seen in the mechanical loss data for both the bonded and reference sample at ~30, 150, and 250 K. The two higher temperature peaks (at 150 and 250 K) were possibly caused by suspension losses or surface losses. Suspension losses could arise from friction between the barrel of the sample and the suspension wire or coupling to the suspension clamp. The level of frictional losses that are experienced can be dependent on the polish of the barrel on the sample. It has previously been shown that mechanical loss peaks can be present for ground or inspection polished samples but are not as prominent for super polished samples [53]. The peak at ~30 K originates from dissipation due to phonon-phonon interactions known as Akhieser damping [22,54].

The extracted mechanical loss values of the hydroxide catalysis bond from the reference and bonded sample data, assuming a 74.5 nm thick bond and a 149 nm thick bond, are displayed in Fig. 5. The intrinsic mechanical loss of the bond was found by averaging the loss measured at each of the resonant modes. If the bond is 74.5 nm thick, the loss is 0.09 ± 0.05 at room temperature and decreases to $(7 \pm 2) \times 10^{-4}$ at 20 K. If the bond is thicker, 149 nm, then the loss of the bond is 0.04 ± 0.02 at room temperature

TABLE II. Parameters used for finite element models of two potential sapphire mirror suspension designs [56,57].

	Design A	Design B
Test mass (kg)	21	211
Diameter (mm)	220	500
Thickness (mm)	150	340
Beam radius (mm)	38	90
Bond area of 1 ear (mm × mm)	30 × 80	45 × 136

and $(4 \pm 1) \times 10^{-4}$ at 20 K. The errors shown are a combination of the error in the spread of the bond loss values at several resonant frequencies and the potential error on the Young's modulus value of a bond. The room temperature values are comparable to the values previously found for the mechanical loss of a hydroxide catalysis bond formed between silica substrates [14,55].

V. THERMAL NOISE CALCULATIONS

Finite element models of two possible sapphire mirror suspension designs involving hydroxide catalysis bonding were created using ANSYS in order to calculate the thermal noise contribution of the bonds to a gravitational wave detector. The thermal noise of two hydroxide catalysis bonds on a test mass was calculated. The modelling method used here has been described in detail in Ref. [14]. The designs were chosen to resemble the suspensions in gravitational wave detectors which have current plans to be operated at cryogenic temperatures; design A is a KAGRA type suspension [56], and design B is an Einstein Telescope type suspension [57]. Table II shows the parameters used to create the suspension design models, and Fig. 6 shows images of the modelled masses with the bonded ears.

The laser beam which is used to sense the displacement of the test mass in a gravitational wave detector was modelled as a Gaussian pressure wave applied to the front surface of the mass with amplitude F_0. This pressure elastically deforms the mass, hydroxide catalysis bond, and ear. Using the energy density of the deformation of the bonds, ϵ, the thermal noise arising from the bonds can be calculated from Ref. [58],

$$S_x(f) = \frac{2k_B T W_{\mathrm{diss}}}{\pi^2 f^2 F_0^2}, \tag{6}$$

where

$$W_{\mathrm{diss}} = 2\pi f \int_{\mathrm{vol}} \epsilon(x,y,z)\phi_{\mathrm{bond}}(x,y,z)dV, \tag{7}$$

where k_B is Boltzmann's constant, T is the temperature, f is the frequency, and W_{diss} is the power dissipated in the bond due to the applied force.

The largest loss values measured for the bond at low temperature, 7×10^{-4} at 20 K and 5×10^{-4} at 10 K, were used in the models in order to give an upper limit of the thermal noise contribution from the bond. The potential range in loss values considering the accuracy of the Young's modulus of the bond is indicated in the error of the thermal noise values presented. The thermal noise arising from the hydroxide catalysis bonds at a frequency of 100 Hz was calculated at 20 K for design A and found to be $(4.8 \pm 1.2) \times 10^{-23}$ m/$\sqrt{Hz}$. The thermal noise of the bonds at a frequency of 10 Hz was calculated at a temperature of 10 K for design B, this gave a thermal noise level of $(3.1 \pm 0.8) \times 10^{-24}$ m/$\sqrt{Hz}$. These results are shown in Table III. The thermal noise arising from the bonds in design B is less than the thermal noise arising from

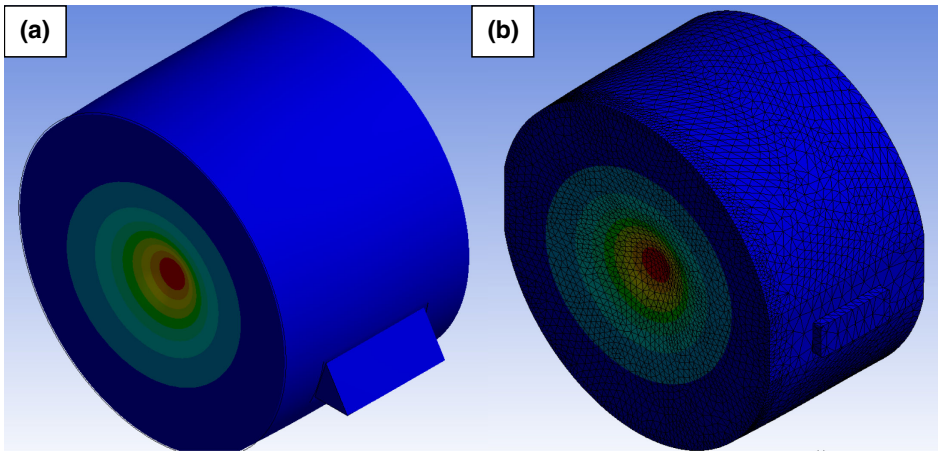

FIG. 6. Finite element model showing the deformation of a test mass and two hydroxide catalysis bonded ears caused by a Gaussian pressure wave. The color indicates the amplitude of the deformation, blue showing the minimum and red showing maximum. (a) Design A, (b) design B showing the finite element mesh. The deformation of the bonds themselves (not visible here) is used to extract the strain energy and therefore calculate the bond thermal noise.

TABLE III. Thermal noise results for KAGRA and the Einstein Telescope design at their operational frequency and cryogenic temperatures. The thermal noise requirement is assumed to be 10% of the thermal noise budget [56,57].

	Design A	Design B
Frequency (Hz)	100	10
Temperature (K)	20	10
Bond loss	7×10^{-4}	5×10^{-4}
Maximum bond thermal noise requirement per test mass $(\mathrm{m}/\sqrt{Hz})$	5×10^{-22}	5×10^{-22}
Calculated expected thermal noise per test mass $(\pm 25\%)(\mathrm{m}/\sqrt{Hz})$	4.8×10^{-23}	3.1×10^{-23}

the bonds in design A as there is a greater distance between the bond area and the location at which the laser beam contacts the front surface of the mass and the radius of the laser beam is larger, therefore resulting in a lower pressure being exerted on the mass. The maximum allowed bond thermal noise was calculated assuming the same requirement set for the aLIGO design, the thermal noise for any component must be less than 10% of the whole thermal noise budget at 100 Hz [59], where the thermal noise budgets for KAGRA at 100 Hz and ET at 10 Hz are used as examples and taken from Refs. [56] and [57], respectively. The interferometer layout is assumed to be the same as for aLIGO with two arms and Fabry-Perot cavities (therefore four masses) in order to calculate the thermal noise requirement per test mass.

VI. DISCUSSION AND SUMMARY

The first measured values for the mechanical loss of a hydroxide catalysis bond created between sapphire substrates was found for several resonant modes. At room temperature, the mechanical loss was found to be between $(0.04\text{–}0.09) \pm 0.05$. This is similar in magnitude to the loss of a hydroxide catalysis bond created between fused silica substrates at room temperature [14]. The decrease of the mechanical loss of the bond with temperature is a desirable feature for cryogenically cooled gravitational wave detectors. At 20 K, which is the operational temperature for KAGRA [15,16], the mechanical loss of a hydroxide catalysis bond falls to a value between $(4\text{–}7 \pm 3) \times 10^{-4}$. At 10 K, the current design operational temperature for the Einstein Telescope, the bond loss falls to a level between $(2\text{–}5 \pm 2) \times 10^{-4}$.

Thermal noise calculations were made for two potential sapphire mirror suspension designs. It has been demonstrated that a sapphire mirror could be suspended with the aid of hydroxide catalysis bonds in such a way that the thermal noise of the bonds meets the noise requirement of gravitational wave detectors. For example, the use of hydroxide catalysis bonding in KAGRA would not prevent it from reaching its design sensitivity which is at a level similar to that of aLIGO. Moreover, the ET's sensitivity, which is aimed to be close to 2 orders of magnitude better than aLIGO at 10 Hz, would not be compromised by the use of these bonds. This is an important result demonstrating the potential of using hydroxide catalysis bonds in future advanced gravitational wave detectors with crystalline materials. The use of these bonds aid in the creation of low mechanical loss suspensions at low temperature contributing to an improved detector sensitivity, which will allow for the detection of more gravitational wave signals from astrophysical sources.

ACKNOWLEDGMENTS

The authors would like to thank the UK Science and Technology Facilities Council (Grants No. ST/I001085/1, No. ST/J000361/1, and No. ST/L000946/1), the University of Glasgow, the Scottish Funding Council, the Royal Society (Grants No. DH120021 and No. RG120367), JSPS KAKENHI (Grant No. 24244031), and the German Science Foundation DFG under contract SFB for financial support. Also, our thanks go to our colleagues in the GEO600 and LIGO Scientific Collaboration for their interest in this area. A. A. van Veggel is the holder of a Royal Society Dorothy Hodgkin Fellowship and research grant. This work has been carried out with the support of the European Commission under the Framework Program 7 "People" and project ELiTES (Grant No. 295153).

[1] LIGO Scientific and Virgo Collaborations, Phys. Rev. Lett. **116**, 061102 (2016).
[2] LIGO Scientific and Virgo Collaborations, Phys. Rev. Lett. **116**, 241103 (2016).
[3] G. M. Harry *et al.*, Classical Quantum Gravity **27**, 084006 (2010).
[4] J. Aasi *et al.*, Classical Quantum Gravity **32**, 074001 (2015).
[5] H. Lück *et al.*, J. Phys. Conf. Ser. **228**, 012012 (2010).
[6] C. Affeldt *et al.*, Classical Quantum Gravity **31**, 224002 (2014).
[7] Virgo Collaboration, Virgo document number VIR-0027A-09, 2009.
[8] F. Acernese *et al.*, Classical Quantum Gravity **32**, 024001 (2015).
[9] M. Pitkin, S. Reid, S. Rowan, and J. Hough, Living Rev. Relativ. **14**, 13 (2011).

[10] A. Ageev, B. C. Palmer, A. De Felice, S. D. Penn, and P. R. Saulson, Classical Quantum Gravity **21**, 3887 (2004).
[11] G. M. Harry *et al.*, Classical Quantum Gravity **24**, 405 (2007).
[12] A. Cumming *et al.*, Classical Quantum Gravity **29**, 035003 (2012).
[13] S. Rowan, S. Twyford, J. Hough, D. Gwo, and R. Route, Phys. Lett. A **246**, 471 (1998).
[14] L. Cunningham *et al.*, Phys. Lett. A **374**, 3993 (2010).
[15] K. Somiya *et al.*, Classical Quantum Gravity **29**, 124007 (2012).
[16] Y. Aso, Y. Michimura, K. Somiya, M. Ando, O. Miyakawa, T. Sekiguchi, D. Tatsumi, and H. Yamamoto, Phys. Rev. D **88**, 043007 (2013).
[17] M. Punturo *et al.*, Classical Quantum Gravity **27**, 194002 (2010).
[18] S. Hild *et al.*, Classical Quantum Gravity **28**, 094013 (2011).
[19] ET Science Team, ET document number ET-0106C-10, 2011.
[20] S. Rowan, J. Hough, and D. Crooks, Phys. Lett. A **347**, 25 (2005).
[21] R. Nawrodt, S. Rowan, J. Hough, M. Punturo, F. Ricci, and J.-Y. Vinet, Gen. Relativ. Gravit. **43**, 593 (2011).
[22] V. B. Braginsky, *Systems with Small Dissipation* (University of Chicago, Chicago, 1985).
[23] L. Ju, M. Notcutt, D. Blair, F. Bondu, and C. Zhao, Phys. Lett. A **218**, 197 (1996).
[24] D. Blair, F. Cleva, and C. Man, Opt. Mater. **8**, 233 (1997).
[25] T. Uchiyama *et al.*, Phys. Lett. A **261**, 5 (1999).
[26] J. Franc, N. Morgado, R. Flaminio, R. Nawrodt, I. Martin, L. Cunningham, A. Cumming, S. Rowan, and J. Hough, arXiv:0912.0107.
[27] B. Barish *et al.*, IEEE Trans. Nucl. Sci. **49**, 1233 (2002).
[28] T. Suzuki *et al.*, J. Phys. Conf. Ser. **32**, 309 (2006).
[29] A. Dari, F. Travasso, H. Vocca, and L. Gammaitoni, Classical Quantum Gravity **27**, 045010 (2010).
[30] N. Beveridge *et al.*, Classical Quantum Gravity **28**, 085014 (2011).
[31] N. Beveridge, A. Van Veggel, L. Cunningham, J. Hough, I. Martin, R. Nawrodt, S. Reid, and S. Rowan, Classical Quantum Gravity **30**, 025003 (2012).
[32] R. Douglas, A. van Veggel, L. Cunningham, K. Haughian, J. Hough, and S. Rowan, Classical Quantum Gravity **31**, 045001 (2014).
[33] K. Haughian, R. Douglas, A. van Veggel, J. Hough, A. Khalaidovski, S. Rowan, T. Suzuki, and K. Yamamoto, Classical Quantum Gravity **32**, 075013 (2015).
[34] P. G. Murray, I. W. Martin, L. Cunningham, K. Craig, G. D. Hammond, G. Hofmann, J. Hough, R. Nawrodt, D. Reifert, and S. Rowan, Classical Quantum Gravity **32**, 115014 (2015).
[35] G. Hofmann *et al.*, Classical Quantum Gravity **32**, 245013 (2015).
[36] D.-H. Gwo, S. Wang, K. Bower, D. Davidson, P. Ehrensberger, L. Huff, E. Romero, M. Sullivan, K. Triebes, and J. Lipa, Adv. Space Res. **32**, 1401 (2003).
[37] D.-H. Gwo, in *SPIE's International Symposium on Optical Science, Engineering and Instrumentation, International Society for Optics and Photonics, San Diego, CA, USA, 1998* (SPIE, 1998), p. 136.
[38] D.-H. Gwo, U.S. Patent 6,284,085 (2001).
[39] E. Elliffe, J. Bogenstahl, A. Deshpande, J. Hough, C. Killow, S. Reid, D. Robertson, S. Rowan, H. Ward, and G. Cagnoli, Classical Quantum Gravity **22**, S257 (2005).
[40] S. Reid, G. Cagnoli, E. Elliffe, J. Faller, J. Hough, I. Martin, and S. Rowan, Phys. Lett. A **363**, 341 (2007).
[41] A. A. van Veggel and C. J. Killow, Adv. Opt. Technol. **3**, 293 (2014).
[42] R. K. Iler, *The Chemistry of Silica: Solubility, Polymerization, Colloid and Surface Pro Perties, and Biochemistry* (Wiley, New York, 1979).
[43] H. Kim and T. Schmitz, Precis. Eng. **37**, 23 (2013).
[44] E. J. Elliffe, Ph. D. thesis, University of Glasgow, 2005.
[45] H. Armandula *et al.*, LIGO document number E050228-v4, 2013.
[46] P. G. Murray, Ph. D. thesis, University of Glasgow, 2008.
[47] H. J. Pain, *The Physics of Vibrations and Waves* (Wiley, New York, 2005).
[48] T. Goto, O. L. Anderson, I. Ohno, and S. Yamamoto, J. Geophys. Res. **94**, 7588 (1989).
[49] P. Sneddon, S. Bull, G. Cagnoli, D. Crooks, E. Elliffe, J. Faller, M. Fejer, J. Hough, and S. Rowan, Classical Quantum Gravity **20**, 5025 (2003).
[50] G. Parker, *Encyclopedia of Materials: Science and Technology* (Elsevier, New York, 2001), p. 2398.
[51] A. Korsunsky, *Encyclopedia of Materials: Science and Technology* (Pergamon, Oxford, 1986), p. 2398.
[52] G. M. Harry *et al.*, Classical Quantum Gravity **19**, 897 (2002).
[53] D. Heinert, Gravitational Wave Advanced Detector Workshop, Takyama, Japan, 2014 (unpublished).
[54] K. Kunal and N. R. Aluru, Phys. Rev. B **84**, 245450 (2011).
[55] K. Haughian, Ph. D. thesis, University of Glasgow, 2012.
[56] K. Yamamoto, 6th Einstein Telescope Symposium, Lyon, Frand, 2014 (unpublished).
[57] ET Science Team, ET technical document number ET-0106C-10, 2011.
[58] Y. Levin, Phys. Rev. D **57**, 659 (1998).
[59] P. Fritschel *et al.*, LIGO document number T-010075-00-D, 2001.